Phase analysis of uranium oxides after reaction with stainless steel components and ZrO2 at high temperature by XRD, XAFS, and SEM/EDX

doi: 10.1016/j.jnucmat.2019.03.055

Manuscript for *Journal of Nuclear Materials*

Title:

Phase analysis of uranium oxides after reaction with stainless steel components and ZrO_2 at high temperature by XRD, XAFS, and SEM/EDX

Authors:

Daisuke Akiyama[*a], Hidenori Akiyama[a], Akihiro Uehara[b, c], Akira Kirishima[a], and Nobuaki Sato[a]

Affiliation:

[a] *Institute of Multidisciplinary Research for Advanced Materials, Tohoku University, 1-1 Katahira, 2, Aoba, Sendai, 980-8577, Japan*

[b] *Division of Nuclear Engineering Science, Research Reactor Institute, Kyoto University, 2-1010, Asashironishi, Kumatori, Osaka, 590-0494, Japan*

[c] *National Institute of Radiological Sciences, National Institutes for Quantum and Radiological Science and Technology, 4-9-1, Anagawa, Inage, Chiba, 263-8555, Japan*

Footnotes:

*Corresponding author,

Text pages	**21 (excluding previous and this page)**
Tables	**1**
Figures	**7**
Corresponding author	**Daisuke Akiyama**
Address	**Institute of Multidisciplinary Research for Advanced Materials, Tohoku University, 1-1 Katahira 2-chome, Aoba-ku, Sendai 980-8577, Japan**
Tel	**+81-22-217-5141**
Fax	**+81-22-217-5141**
Email	**d.akiyam@tohoku.ac.jp**

22

23

Abstract

In the Fukushima Daiichi nuclear power station accident in March 2011, fuel debris was formed when fuel materials reacted with various structural materials in reactor core. Fuel debris retrieval is expected to start in 2021 for decommissioning of the damaged plants. To perform this activity safely, it is necessary to know the properties of the fuel debris. In this study, we investigated the reaction of UO_2, stainless steel (SS) components, and ZrO_2 at high temperature under oxidizing and reducing conditions, and determined the valence state of uranium in the products, such as $CrUO_4$ and $(Fe_x, Cr_{1-x})UO_4$, by X-ray absorption near edge structure (XANES) spectroscopy. Mixed powders of UO_2 and SS, Fe, and/or Cr were heated in Ar + 2% O_2 (oxidizing condition) or Ar + 10% H_2 (reducing condition) at a flow rate of 20 mL/min for 2 h at 1473 or 1673 K. After heat treatment, the phase relation of the products was analyzed by powder X-ray diffraction and scanning electron microscopy with energy-dispersive X-ray spectroscopy. Under reducing conditions, UO_2 did not react with SS, Fe, Cr, or ZrO_2. In contrast, under oxidizing conditions, UO_2 reacted with SS and Cr to form $CrUO_4$ or $(Fe_x, Cr_{1-x})UO_4$ at 1473 and 1673 K. When the UO_2 and Fe mixture was heated under oxidizing conditions, the Fe_2O_3 phase coexisted with U_3O_8 at 1473 K, whereas $FeUO_4$ formed at 1673 K. When the UO_2, Fe, and Cr mixtures were heated at 1473 K under the oxidizing condition, the molar ratio of Fe/Cr in the $(Fe_x, Cr_{1-x})UO_4$ phase corresponded to the initial molar ratio in the sample. As the iron content of these samples increased, all three lattice parameters of $(Fe_x, Cr_{1-x})UO_4$ approached those of $FeUO_4$. XANES spectra revealed that the oxidation state of uranium in $CrUO_4$ and $(Fe_x, Cr_{1-x})UO_4$

is pentavalent.

Keywords: Uranium oxide; Stainless steel; Iron; Chromium; XAFS; XANES; XRD; SEM/EDX; Fukushima Daiichi Nuclear Power Plant; Fuel debris

High lights

- UO_2 reacted with chromium and SS at 1473 and 1673 K under oxidizing conditions, forming $CrUO_4$ and $(Fe_x, Cr_{1-x})UO_4$.
- UO_2 reacted with iron at 1673 K under oxidizing conditions, forming $FeUO_4$.
- Chromium promoted the formation of $(Fe_x, Cr_{1-x})UO_4$ in the UO_2–SS system.
- When zirconium was coexisted with the UO_2-SS, formation of $(Fe_x, Cr_{1-x})UO_4$ was suppressed.
- The oxidation state of uranium in $CrUO_4$ and $(Fe_x, Cr_{1-x})UO_4$ was pentavalent.

1. Introduction

A severe accident occurred at Fukushima Daiichi nuclear power plant (NPP) in Japan, which is operated by the Tokyo Electric Power Company, in March 2011, in which the fuel reacted with the cladding material at high temperature, and the reactor core melted down. It was suggested that the nuclear fuel materials reacted with not only the fuel cladding but also core structural materials, the concrete pedestal, and sea salt introduced by emergency cooling using seawater. These components might be present in the fuel debris in the pressure vessel and/or on the concrete pedestal [1].

The pressure vessel and containment vessel in a boiling water reactor are normally filled with nitrogen gas. In a loss-of-coolant accident, hydrogen generated by the reaction between the zircaloy cladding and H_2O coolant at high temperature would create reducing conditions

around the fuel debris. Then, the hydrogen gas caused explosion in units 1, 3 and 4 of Fukushima Daiichi NPP. After that, in units 1 and 2, concentration of oxygen in containment vessel has not changed approximately 0%, on the other hand, in unit 3, it was reported as a plant condition report of July 2012 by TEPCO, that the O_2 concentration of unit 3 was approximately 11% due to damage of the containment vessel [2]. Therefore, it is necessary to assess the reaction of fuel materials and core structural materials, the concrete pedestal, and sea salt at high temperature under both reducing and oxidizing conditions. For understanding the characteristics of fuel debris generated in Fukushima Daiichi NPP, the knowledge from studying the core samples from Three Mile Island Unit-2 (TMI-2, pressurized water reactor [PWR]) is important [3-6]. However, there are the differences in reactor type and in the circumstances during melting cores. Since the debris sampling from 1F is still under consideration, several types of simulated fuel debris were synthesized and used for laboratory studies [7, 8]. The interaction between corium and structural materials in oxidizing conditions was also investigated [9-11]. We have reported the phase relation between UO_2 and ZrO_2 at 1473 K resulted in the formation of a solid solution of $U(Zr)O_2$ by phase analysis [12]. Kitagaki et al. investigated thermodynamic evaluation on fuel debris in the UO_2–ZrO_2 system and the molten core concrete interaction [13]. Furthermore, the leaching of fission products (FPs) and actinides into seawater has been performed using UO_2–ZrO_2 debris synthesized by heat treatment at 1473 K. Here, FPs and actinides in the UO_2–ZrO_2 were produced by neutron irradiation of a solid solution of $U(Zr)O_2$ [14, 15]. On the other hand, the leaching tests for actinide elements were conducted by doping a $U(Zr)O_2$ solid solution with Np, Am, and Pu tracers; our previous study revealed only very limited

93 leaching of the actinide tracers into seawater and the reducing effect of the leached actinides
94 by Zr(IV) dissolution in the UO_2 crystal structure [16, 17]. Stainless steel (SS) was used as a
95 core structural material and would have reacted with most of the solidified fuel material. We
96 have reported that UO_2 reacted with SS and formed $(Fe_x, Cr_{1-x})UO_4$ at 1473 K under
97 oxidizing conditions [18]. On the other hand, metal monouranates, MUO_4, have been
98 interested due to their importance in actinide chemistry and nuclear technology. So the
99 characteristics of these compound are frequently reported [19-29]. For example, the reaction
100 behavior of UO_2 and metals, and the properties of the reactants, such as $CrUO_4$, $FeUO_4$, and
101 $MgUO_4$, have been studied recently [29]. In this previous study, oxidation states of uranium
102 in $FeUO_4$ or $CrUO_4$ was confirmed pentavalent. Petrrov et al. reported that in the U-Fe-O
103 system and U-Zr-Fe-O system, samples melted with quenching in air. Then, $FeUO_4$, UO_2,
104 U_3O_8, Fe_2O_3 and Fe_3O_4 phases were observed in the both systems [35, 39]. Furthermore,
105 thermodynamic measurement and characterization of $UFeO_4$ were reported [36]. D. Labroche
106 et al. indicted that the formation enthalpy of $FeUO_4$ was -25.2 ± 0.6 kJ/mol at 298.15 K, and
107 the enthalpy increased with temperature. In addition, the $CrUO_4$ phase was insoluble in hot
108 50% HNO_3, then it is important to obtain the forming condition for planning chemical
109 treatment after retrieval fuel debris. [31]. However, the reactions of UO_2 and alloys such as
110 SS and forming condition of $(Fe_x, Cr_{1-x})UO_4$ were not clear. Following the earlier study [18],
111 it is necessary to know the phase relation among UO_2, Fe, and Cr at high temperature to
112 understand the reaction mechanism between UO_2 fuel and SS. Furthermore, the phase
113 relation among UO_2, SS, and ZrO_2 was also studied as a realistic system for the fuel debris
114 of Fukushima NPP. Because Zr is a major component of fuel cladding, UO_2, SS, and Zr

should interact in the damaged reactors. The purpose of this paper is to investigate the reactions between UO_2, Fe, Cr, SS, and ZrO_2. The compounds prepared were analyzed by X-ray powder diffraction spectroscopy (XRD) and scanning electron microscopy- Energy Dispersive X-ray Spectroscopy (SEM-EDX). Oxidation state of uranium in $(Fe_x, Cr_{1-x})UO_4$ was confirmed based on X-ray absorption near edge structure (XANES) of U L_{III} edge.

2. Experimental

2.1. Materials

UO_2 was prepared by H_2 reduction of U_3O_8 at 1273 K. The formation of UO_2 was confirmed by an X-ray diffraction (XRD) measurement. Iron powder (the content of the main component was 99.95%, <60 mesh) and chromium powder (the content of the main component was 99.5%, <100 mesh) were purchased from Nilaco Corporation and Sigma-Aldrich, respectively. Cr_2O_3 (the content of the main component was 99.9%) and ZrO_2 (the content of the main component was 98.0%) were purchased from Mitsuwa Chemical Corporation and Wako Pure Chemicals Ind., Ltd. SUS304 SS composed of 68.77% iron, 18.71% chromium, 11.09% nickel, and minor elements was purchased from Nilaco Corporation.

UO_3 was synthesized by heating $UO_2(NO_3)_2 \cdot 6H_2O$ at 773 K with Ar + 2% O_2 for 5 h.

2.2. Heat treatment

2.2.1. UO_2–Fe system

UO_2 powder was mixed with Fe in a molar ratio of 1:1 and ground in an agate mortar. A quartz or alumina boat containing this mixture was placed in the center of a reaction tube made of quartz or alumina. After the reaction tube was evacuated, it was refilled with Ar + 10% H_2 or Ar + 2%O_2, which were introduced to obtain reducing or oxidizing conditions, respectively. Then each sample was heated to 1473 or 1673 K at a heating rate of 17 K/min up to 1273 K and 7 K/min from 1273 to 1473 or 1673 K. The target temperature was maintained, and Ar + 10% H_2 gas or Ar + 2% O_2 gas was added at 1473 or 1673 K to obtain the reducing or oxidizing condition, respectively. After heat treatment, the samples were cooled at a cooling rate of 17 K/min to 873 K and furnace cooled to room temperature. After cooling, they were removed from the reaction tube for phase analysis.

2.2.2. UO_2–Cr system

UO_2 powder was mixed with Cr powder in a molar ratio of 1:1 and ground in an agate mortar. Alternatively, U_3O_8 was mixed with Cr_2O_3 in a molar ratio of 2:3 and ground in an agate mortar. The UO_2–Cr mixture was heated by the same procedure as that used for the UO_2–Fe system. The U_3O_8–Cr_2O_3 mixture was also heated by almost the same process except that ultrapure Ar was used during heating at 1473 K for 2 h.

2.2.3. UO_2–Fe–Cr system

158 UO_2 powder was mixed with Fe and Cr powders. The molar ratio of UO_2/(Fe + Cr) was
159 kept at 1, whereas the molar ratio of Fe/(Fe + Cr) was varied from 0.1 to 0.9. The molar
160 ratio of SUS304, the SS used in this study, was approximately 0.79. The UO_2–Fe–Cr
161 mixtures were heated by the same procedure as that used for UO_2–Fe system.
162
163 2.2.4. UO_2–Zr–SS system
164 UO_2 was mixed with SS powder or SS and ZrO_2 powders. The molar ratio of (UO_2 +
165 ZrO_2)/ (Fe in SS) was maintained at 1. The molar ratio of UO_2/ (UO_2 + ZrO_2) was 0.5 and
166 1. The UO_2–Fe–Cr mixtures were heated by same process as that used for the UO_2–Fe
167 system.
168
169 Table 1 summarizes the composition of the initial samples and the heating conditions.
170 [Table 1]
171
172 2.3. Phase analysis
173
174 The XRD patterns of the products were measured using a Rigaku MiniFlex 600
175 diffractometer with Cu Kα irradiation at 40 kV and 15 mA. The diffraction data were
176 collected from 20° to 120° (2θ) with a step interval of 0.02° at a scan rate of 20°/min. The
177 phase of the products was determined by matching the measured patterns with XRD
178 patterns from the Inorganic Crystal Structure Database [32]. The lattice parameters of the
179 compounds were calculated using PDXL2 (Rigaku).
180 The samples were examined by scanning electron microscopy (SEM, SU1510, Hitachi

Corp.) with energy-dispersive X-ray spectroscopy (EDX, EMAX EX-250, XACT, Horiba Corp.) to observe the microstructure and analyze the elemental composition.

The oxidation state of U in the products was determined by X-ray absorption near edge structure (XANES) spectroscopy. X-ray absorption fine structure (XAFS) spectra were collected at SPring-8 (Japan Synchrotron Radiation Research Institute, Hyogo, Japan) using BL01B1 beamline. UO_2 and UO_3 were used as standard tetravalent and hexavalent U materials, respectively.

3. Results and discussion

3.1. Temperature dependence of phase relation in the UO_2–Fe system

Fig. 1 shows the XRD patterns of the UO_2−Fe (1:1) samples before and after heat treatment at 1473 and 1673 K for 2 h under the reducing and oxidizing conditions. No significant change was observed in the diffraction patterns obtained after heat treatment under the reducing condition at either temperature up to for 8h, indicating that UO_2 did not react with Fe up to 1673 K under the reducing condition. When this sample was heated under the oxidizing condition, UO_2 and Fe were oxidized to U_3O_8 and Fe_2O_3 at 1473 K; in contrast, UO_2 and Fe were oxidized to U_3O_8, Fe_3O_4, and $FeUO_4$ was formed at 1673 K. The result at 1673K almost agreed with the phase relation of samples that melted with quenching in the U-Fe-O system in air [35]. Then, these uranium and iron oxides reacted and formed the $FeUO_4$ phase at 1673 K by the following reaction.

Synthesis of $FeUO_4$ has been reported in a previous study [29, 31, 36], in which attempts to synthesize $FeUO_4$ by regular solid-state synthesis, coprecipitation, and hydrothermal methods did not success. Successful synthesis was finally obtained by heat treatment of stoichiometric mixtures of (UO_3, FeO), (U_3O_8, Fe_3O_4), or (UO_2, U_3O_8, and Fe_2O_3) in a vacuum-sealed quartz tube at 1223–1423 K for 2 weeks by the following reaction [29, 31, 36].

$$UO_3 + FeO \rightarrow FeUO_4 \quad (1)$$

$$\frac{1}{3}U_3O_8 + \frac{1}{3}Fe_3O_4 \rightarrow FeUO_4 \quad (2)$$

$$\frac{1}{4}U_3O_8 + \frac{1}{4}UO_2 \ \frac{1}{2}Fe_2O_3 \rightarrow FeUO_4 \quad (3)$$

This indicates that $FeUO_4$ was formed from the mixture of uranium and iron oxides with different oxidation states to compensate their valence state each other by heat treatment. In the present study, at 1473K under oxidizing condition, U_3O_8 didn't react with Fe_2O_3, on the other hand, at 1673K under oxidizing condition,U_3O_8 reacted with Fe_3O_4 and $FeUO_4$ was formed by the reaction eq.(2). U_3O_8 and Fe_3O_4 phase remained because heating time was shorter than previous studies and/or it was different from temperature and open or closed system [29, 31, 36]. Fe_3O_4 is more stable than Fe_2O_3 above 1653K in air [33]. Then these results indicated that the reaction eq (2) could progress in the UO_2-Fe system under oxidizing condition at the temperature range where U_3O_8 and Fe_3O_4 were stable.

[Fig.1]

3.2 Temperature dependence of the phase relation in the UO_2–Cr system

In the UO_2–Cr system, UO_2 and Cr did not react under the reducing condition at 1473 or 1673 K up to for 8h, as shown in Fig. 2a. Under the oxidizing condition, UO_2 and Cr were oxidized to U_3O_8 and Cr_2O_3 at 1473 and 1673 K. Furthermore, the $CrUO_4$ phase was observed at both 1473 and 1673 K, as shown in Fig. 2b. The $CrUO_4$ phase was formed with heating time at 1473K, while U_3O_8 phase decreased. To confirm the formation reaction of $CrUO_4$, U_3O_8 was mixed with Cr_2O_3 in a molar ratio of 2:3 and heated under an ultrapure Ar atmosphere at 1473 K for 2 h. After heat treatment, the peaks for $CrUO_4$ was observed in the XRD pattern of the product. Some of the U_3O_8 was reduced to U_4O_9, and Cr_2O_3 remained. This result suggested that $CrUO_4$ was formed by the following reaction.

$$\frac{1}{3}U_3O_8 + \frac{1}{2}Cr_2O_3 \rightarrow CrUO_4 + \frac{1}{12}O_2 \quad (2)$$

It was confirmed that $CrUO_4$ was formed in a wide temperature range in the UO_2–Cr system under the oxidizing condition, as shown in Fig. 2b, whereas $FeUO_4$ was formed only at 1673 K in the UO_2–Fe system, as shown in Fig. 1b. The typical peak of $CrUO_4$ is indicated by an arrow in Fig. 2b. The reaction between U_3O_8 and Cr_2O_3 occurs in the temperature region from 1128 to 1293K and $CrUO_4$ phase was observed below 1873K [19, 31]. These results agree well with published data. From the above discussion, it is concluded that the formation of $CrUO_4$ is more favorable than that of $FeUO_4$ because of the stability of trivalent chromium than that of trivalent iron.

246

247 [Fig. 2]

248

249 3.3 Temperature dependence of phase relation in the UO_2–SS and UO_2–ZrO_2–SS systems

250

251 In the UO_2–SS system, uranium oxide and SS phases did not change under the reducing
252 condition at 1473 and 1673 K up to for 8h, as observed in the UO_2–Fe system. It was
253 reported that they were dissolved in each other when UO_2 and SS were in melted state,
254 while these compounds were not reacted each other at temperature below UO_2 melting
255 point 3120 K [37, 38]. Under the oxidizing condition, UO_2 and SS were oxidized to U_3O_8
256 and $(Fe, Cr)_3O_4$ at 1473 and 1673 K. Furthermore, the $(Fe_x, Cr_{1-x})UO_4$ phase was observed
257 at both temperatures. Peaks for the $(Fe_x, Cr_{1-x})UO_4$ phase was increased with increasing
258 heating time at 1473K, while peaks for the U_3O_8 phase decreased. It was observed that Cr,
259 which is the second most abundant component in the SS used in this study, promoted the
260 formation of the $(Fe_x, Cr_{1-x})UO_4$ phase, as it did in the UO_2–Fe–Cr system.
261 In the UO_2–ZrO_2–SS system, the $(Fe_x, Cr_{1-x})UO_4$ phase was also formed with heating
262 time, however, the peak intensities of $(Fe_x, Cr_{1-x})UO_4$ phase were lower than those in the
263 UO_2–SS system because some of the UO_2 reacted with ZrO_2 and formed a $(U, Zr)O_2$ solid
264 solution. The crystal structure of ZrO_2 changes reversibly from monoclinic crystal structure
265 at room temperature to tetragonal one at 1343 K [34]. After heat treatment, ZrO_2 existed as
266 the tetragonal phase at room temperature because the tetragonal ZrO_2 phase was stabilized
267 by the formation of a solid solution with UO_2 at high temperature and the phase transition

from tetragonal to monoclinic did not occur during cooling. The result at 1673K were almost consistent with the phase relation of samples which melted with quenching cooling in the U-Zr-Fe-O system in air [39].

On the other hand, it was confirmed that $CrUO_4$ and (Fe, Cr)UO_4 were formed in a wide temperature range in the UO_2–Cr and UO_2–SS systems under the oxidizing condition, whereas little of the simple $FeUO_4$ phase was formed in the UO_2–Fe system. The results indicated that the presence of chromium promoted the formation of $(Fe_x, Cr_{1-x})UO_4$ in the UO_2–SS system. However, when zirconium was coexistent with the UO_2-SS, formation of $(Fe_x, Cr_{1-x})UO_4$ was suppressed by formation of the (U, Zr)O_2 solid solution.

[Fig. 3]

3.4. Characterization of the (Fe, Cr)UO_4 phase

It was confirmed that the (Fe, Cr)UO_4 phase was formed at 1473 and 1673 K under the oxidizing condition in the UO_2–SS system. To examine the (Fe, Cr)UO_4 phase further, UO_2 was mixed with Fe and Cr and heated at 1473 K for up to 24 h under the oxidizing condition. In this case, $(Fe_x, Cr_{1-x})UO_4$ (x = 0.25–0.9) was formed in the UO_2–Fe–Cr system as well as in the UO_2–SS system. Fig. 4 shows the lattice parameters of the $(Fe_x, Cr_{1-x})UO_4$ obtained in the UO_2–Fe–Cr system by heat treatment at 1473 K for 24 h, $FeUO_4$ obtained in the UO_2–Fe system by heat treatment at 1673 K for 2 h, and $CrUO_4$ obtained in the UO_2–Cr system by heat treatment at 1473 K for 24 h. The lattice parameters of the $(Fe_x, Cr_{1-x})UO_4$ phase obtained in the UO_2–SS system are also shown in Fig. 4 for comparison.

The lattice parameters of $FeUO_4$ and $CrUO_4$ are close to the literature values. All the lattice parameters of $(Fe_x, Cr_{1-x})UO_4$ in the UO_2–Fe–Cr and UO_2–SS systems are between those of $CrUO_4$ and $FeUO_4$. The lattice parameters (a, b, and c) of $(Fe_x, Cr_{1-x})UO_4$ increase in proportion to the Fe/Cr ratio. This result suggests that the $(Fe_x, Cr_{1-x})UO_4$ unit cell expands isotopically by random replacement of Fe atoms with Cr atoms.

[Fig. 4]

Fig. 5 shows SEM and X-ray mapping images of the product after heat treatment at 1473 K under the oxidizing condition in the UO_2–SS system. The U and Fe distribution in the sample seem to be heterogeneous, on the other hand, the Cr seems to be homogeneous due to low content of Cr in the sample. The phases were classified into three types according to the U, Fe, and Cr distributions: a uranium oxide phase where U distributed position, a Cr oxide and Fe oxide phase where Fe, Cr, and O distributed same position, and a (Fe, Cr)UO_4 phase where U, Fe, and Cr distributed same position. In addition, Ni, which makes up 11.09% of the SS used here, appeared in the Cr oxide and Fe oxide phases.

This (Fe, Cr)UO_4 phase was also observed in the UO_2–Fe–Cr system. Then, the elemental composition of the (Fe, Cr)UO_4 phase was analyzed by spot analysis. Fig. 6 shows the molar ratio of Fe/Cr in the (Fe, Cr)UO_4 phase in the UO_2-Fe-Cr system and UO_2-SS system. These results indicate that the $(Fe_x, Cr_{1-x})UO_4$ phase in the UO_2–Fe–Cr and UO_2–SS systems is consistent with the lattice parameters obtained by XRD analysis. The experimental results presented in this study revealed that chromium played an important role as a catalyst in

forming the $(Fe_x, Cr_{1-x})UO_4$ phase in the UO_2–Fe–Cr system. The following reactions are proposed as the mechanism for $(Fe_x, Cr_{1-x})UO_4$ phase formation.

$$\frac{1}{3}U_3O_8 + \frac{1}{2}Cr_2O_3 \rightarrow CrUO_4 + \frac{1}{12}O_2 \quad (3)$$

$$CrUO_4 + \frac{1}{12}O_2 + \frac{x}{3}Fe_3O_4 \rightarrow (Fe_x, Cr_{1-x})UO_4 + \frac{x}{2}Cr_2O_3 \quad (4)$$

First, UO_2 and Cr were oxidized to U_3O_8 and Cr_2O_3; then, the $CrUO_4$ forming reaction proceeded, as shown in Eq. (3), at 1473 K. Next, the chromium ion in $CrUO_4$ was replaced with the iron ion in Fe_3O_4, and $(Fe_x, Cr_{1-x})UO_4$ and Cr_2O_3 were formed, as shown in Eq. (4). Therefore, Cr_2O_3 reacted continuously with U_3O_8 as long as they remained. As shown in Fig. 6, the molar ratios of Fe/Cr observed by EDX analysis of the $(Fe_x, Cr_{1-x})UO_4$ phase in the synthesized samples were proportional to those in the starting materials; therefore, the coefficient x in Eq. (4) depends on the mixture ratio of Fe/Cr before heat treatment. Up to now, the reaction of fuel materials and core structural materials was often assessed in U-Fe-O system or U-Zr-Fe-O system [9-11]. However, it is found that the phase relation of fuel materials and core structural materials were significantly affected by chromium under oxidizing conditions even if it is small amount. The existence of chromium must be considered when the fuel debris in unit 3 of Fukushima Daiichi NPP, where the O_2 concentration was high, is investigated.

[Fig. 5]

[Fig. 6]

Fig. 7 shows the U L_{III} XANES spectra of standard uranium oxides, $(Fe_x, Cr_{1-x})UO_4$ (x = 0.25, 0.5, 0.75), and the $CrUO_4$ samples. The U L_{III} spectra of UO_2 and UO_3 show absorption edge energies (E_0) of 17162.424 and 17165.700 eV, respectively. These values are consistent with the U^{4+} and U^{6+} oxidation states. $(Fe_x, Cr_{1-x})UO_4$ (x = 0.25, 0.5, 0.75) and $CrUO_4$ show E_0 values between those of UO_2 and UO_3. No significant change was observed in the U L_{III} XANES spectra at any molar ratio of Fe/Cr. The uranium oxidation states of $CrUO_4$ and $FeUO_4$ are reportedly pentavalent according to XANES spectroscopy [10]. In this study, the valence state of $CrUO_4$ is in agreement with that in a previous study, and that of $(Fe_x, Cr_{1-x})UO_4$ is found to be pentavalent regardless of the molar ratio of Fe/Cr.

[Fig. 7]

4. Conclusion

In this study, UO_2 did not react with SS, iron, or chromium under the reducing condition at 1473 and 1673 K. However, under the oxidizing condition, the UO_2 and SS components were oxidized and reacted at 1473 and 1673 K. Some of the UO_2 was oxidized to U_3O_8 at 1473 and 1673 K under the oxidizing condition, whereas the rest of the UO_2 reacted with chromium and SS at 1473 and 1673 K, forming $CrUO_4$ and $(Fe_x, Cr_{1-x})UO_4$. In addition, UO_2 reacted with iron only at 1673 K, forming $FeUO_4$. In the UO_2–ZrO_2–SS system, UO_2 reacted with ZrO_2 and formed a $(U, Zr)O_2$ solid solution, which prevented the formation of $(Fe, Cr)UO_4$. In the ternary system UO_2–Fe–Cr, $(Fe_x, Cr_{1-x})UO_4$ was formed at 1473 K, and

proportional to that in the starting materials. XANES spectra indicated that the oxidation state of uranium in $CrUO_4$ and $(Fe_x, Cr_{1-x})UO_4$ was pentavalent. The results suggest that at the Fukushima Daiichi NPP, molten fuel could react with structural materials consisting of alloys containing chromium to form $(Fe_x, Cr_{1-x})UO_4$ under the oxidizing condition at 1473 K, below which it is known that the molten fuel could not react with iron. Note that zirconium suppresses $(Fe_x, Cr_{1-x})UO_4$ formation.

Acknowledgments

This work was partially supported by the Research Program for CORE lab of "Dynamic Alliance for Open Innovation Bridging Human, Environment and Materials" in "Network Joint Research Center for Materials and Devices." The authors gratefully acknowledge Kazuhisa Matsumoto (Chiba University), Chiya Numako (Chiba University), Yasuko Terada (Japan Synchrotron Radiation Research Institute), Toshiaki Ina (Japan Synchrotron Radiation Research Institute), and Shino Takeda-Homma (National Institute of Radiological Sciences, National Institutes for Quantum and Radiological Science and Technology) for their cooperation in the XANES measurement at SPring-8 under the 2016A1693, 2016B1805 and 2017A1725 programs.

References

[1] (in Japanese) The Evaluation Status of Reactor Core Damage at Fukushima Daiichi Nuclear Power Station Units 1 to 3 [Internet], Tokyo Electric Power Company, Tokyo, Dec. 25, 2017. Available from http://www.tepco.co.jp/press/release/2017/pdf2/171225j0102.pdf.

[2] (in Japanese) The situation in the primary containment vessel based on the result of the gas measurement, Tokyo Electric Power Company, Tokyo, July. 23, 2012. Available from http://www.tepco.co.jp/nu/fukushima-np/images/handouts_120723_06-j.pdf

[3] Broughton JM, Kuan P, Petti DA, Tolman EL. A scenario of the Three Mile Island Unit 2 accident. Nucl Technol. 1989, 87, 34–53.

[4] Olsen CS, Jensen SM, Carlson ER, Cook BA. Materials interactions and temperatures in the Three Mile Island Unit 2 core. Nucl Technol. 1989, 87, 57–94.

[5] Bottomley PD, Coquerelle M. Metallurgical examination of bore samples from the Three Mile Island Unit 2 reactor core. Nucl Technol. 1989, 87, 120–136.

[6] Hofmann P, Hagen SJL, Schanz G, Skokan A. Reactor core materials interactions at very high tempratures. Nucl Technol. 1989, 87, 146–186.

[7] M. Takano, T. Nishi, N. Shirasu, Characterization of solidified melt among materials of UO_2 fuel and B_4C control blade, J. Nucl. Sci. Technol. 51 (7–8) (2014) 859–875.

[8] M. Takano, T. Nishi, N. Shirasu, High temperature reaction between sea salt deposit and $(U,Zr)O_2$ simulated corium debris, J. Nucl. Mater. 443 (2013) 32–39.

[9] BECHTA, S. V., et al. Corrosion of vessel steel during its interaction with molten corium: Part 1: Experimental. Nuclear engineering and design, 236.17 (2006) 1810-1829.

[10] BECHTA, S. V., et al. Corrosion of vessel steel during its interaction with molten corium: Part 2: Model development. Nuclear engineering and design, 236.13 (2006) 1362-1370.

[11] ALMJASHEV, V. I., et al. Eutectic crystallization in the $FeO_{1.5}$–UO_{2+x}–ZrO_2 system. Journal of Nuclear Materials, 389.1 (2009) 52-56.

[12] N. Sato, A. Kirishima, T. Sasaki, Behavior of fuel and structural materials in severely damaged reactors, in: Proceedings of CIMTEC 2014, Advances in Science and Technology, 6th Forum on New Materials, Part B, Trans. Tech. Pub. Inc. (2014) 93–96.

[13] T. Kitagaki, K. Yano, H. Ogino, T. Washiya, Thermodynamic evaluation of the solidification phase of molten core-concrete under estimated Fukushima Daiichi nuclear power plant accident conditions, J. Nucl. Mater. 486 (2017) 206–215.

[14] T. Sasaki, Y. Takeno, A. Kirishima, N. Sato, Leaching test of gamma-emitting Cs, Ru, Zr, and U from neutron-irradiated UO_2/ZrO_2 solid solutions in non-filtered surface seawater, J. Nucl. Sci. Technol. 52 (2015) 147–151.

[15] T. Sasaki, Y. Takeno, T. Kobayashi, A. Kirishima, N. Sato, Leaching behavior of gamma-emitting fission products and Np from neutron-irradiated UO_2–ZrO_2 solid solutions in non-filtered surface seawater, J. Nucl. Sci. Technol. 53 (2016) 303–311.

[16] A. Kirishima, M. Hirano, T. Sasaki, N. Sato, Leaching of actinide elements from simulated fuel debris into seawater, J. Nucl. Sci. Technol. 52 (2015) 1240–1246.

[17] A. Kirishima, M. Hirano, D. Akiyama, T. Sasaki, N. Sato, Study on the leaching behavior of actinides from nuclear fuel debris, J. Nucl. Mater. 502 (2018) 169–176.

[18] D. Akiyama, A. Kirishima, N. Sato, T. Sasaki, Reaction behavior of uranium oxides and structural materials at high temperatures, in: Proceedings of Global 2015 Meeting, 20-24 September 2015, Paris, France, 5373 (2015).

[19] FELTEN, E. J.; JUENKE, E. F.; BARTRAM, S. F, The system Cr_2O_3- UO_2- O_2, Journal of Inorganic and Nuclear Chemistry, 24.7 (1962) 839-845.

[20] Greenblatt, M., R. M. Hornreich, and B. Sharon, Magnetoelectric compounds with two

422 sets of magnetic sublattices, $UCrO_4$ and $NdCrTiO_5$, Journal of Solid State Chemistry, 10.4
423 (1974) 371-376.
424 [21] P. A. G. Ohare, J. Boerio, D. R. Fredrickson and H. R. Hoekstra, Thermochemistry of
425 uranium compounds IX. Standard enthalpy of formation and high-temperature
426 thermodynamic functions of magnesium uranate ($MgUO_4$) A comment on the non-existence
427 of beryllium urinate, J. Chem. Thermodyn., 9 (1977) 963–972.
428 [22] G. C. Allen, A. J. Griffiths and B. J. Lee, X-ray photoelectron spectroscopy of alkaline
429 earth metal uranate complexes, Transition Met. Chem., 3 (1978) 229–233.
430 [23] E. H. P. Cordfunke, A. S. Booij and M. E. Huntelaar, The standard enthalpies of
431 formation of uranium compounds. XV. Strontium urinates, J. Chem. Thermodyn., 31 (1999)
432 1337–1345.
433 [24] D. B. S. Van, M. Verwerft, J. P. Laval, B. Gaudreau, P. G, The local uranium environment
434 in cesium uranates: a combined XPS, XAS, XRD, and neutron diffraction analysis, Allen and
435 W. A. Van, J. Solid State Chem., 166 (2002) 320–329.
436 [25] K.-A. Kubatko, K. Helean, A. Navrotsky and P. C. Burns, Thermodynamics of uranyl
437 minerals: Enthalpies of formation of uranyl oxide hydrates, Am. Mineral., 91 (2006) 658–
438 666.
439 [26] A. V. Soldatov, D. Lamoen, M. J. Konstantinovic, d. B. S. Van, A. C. Scheinost and M.
440 Verwerft, J. Solid State Chem., 180 (2007) 54–61.
441 [27] J. H. Liu, d. B. S. Van and M. J. Konstantinovic, Local structure and oxidation state of
442 uranium in some ternary oxides: X-ray absorption analysis, J. Solid State Chem., 182 (2009)
443 1105–1108.

[28] E. S. Ilton and P. S. Bagus, Surf, XPS determination of uranium oxidation states, Interface Anal., 43 (2011) 1549–1560.

[29] X. Guo, E. Tiferet, L. Qi, J.M. Solomon, A. Lanzirotti, M. Newville, M.H. Engelhard, R.K. Kukkadapu, D. Wu, E.S. Ilton, M. Asta, S.R. Sutton, H. Xu, A. Navrotsky, U(V) in metal uranates: a combined experimental and theoretical study of $MgUO_4$, $CrUO_4$, and $FeUO_4$, Dalton Trans. 45 (2016) 4622–4632.

[30] Collomb, A., et al. Hydrothermal Synthesis of Some Mixed Oxides A 6+ B 3+ O 6 under High Pressures. J. Solid State Chem, 23.3-4 (1978) 315-319.

[31] H.R. Hoekstra, R.H. Marshall, Some uranium-transition element double oxides, Adv. Chem. 71 (1967) 211–227.

[32] G. Bergerhoff, I.D. Brown, in: F.H. Allen, et al. (Eds.), Crystallographic Databases, International Union of Crystallography, Chester, (1987).

[33] W.D.J. Evans, J. White, Equilibrium relationships in the system UO_2-Fe_3O_4-O, Trans. Brit. Ceram. Soc. 63(12) (1964) 705–724.

[34] C. Pascual, P. Duran, Subsolidus phase equilibria and ordering in the system ZrO_2-Y_2O_3, J. Am. Ceram. Soc. 66 (1983) 23–27.

[35] Yu. B. Petrov, Yu. P. Udalov, J. Subrt, S. Bakardjieva, P. Sazavsky, M. Kiselova, P. Selucky, P. Bezdicka, C. Journeau, and P. Piluso, Phase equilibria during crystallization of melts in the uranium oxide-iron oxide system in air", Glass Physics and Chemistry 35(3) (2009) 296-305.

[36] D. Labroche et al. "Thermodynamic Measurement and Characterization of UFeO4 Compound, Proceedings of the 10 International IUPAC Conference, 10-14 April 2000, Julich, Germany (2000) 89-95.

[37] Hodkin, D.J. and Potter, P.E, On the chemical constitution of a molten oxide core of fast breeder reactor, Revue Internationale des Hautes Températures et Réfractaires 17 (1980) 70-81.

[38] H. Kleykamp, Phase equilibria in the UO_2-austenitic steel system up to 3000°C, Journal of Nuclear Materials 247 (1997) 103-107.

[39] Petrov, Y.B. and Udalov, Y.P. and Subrt, J. and Bakardjieva, S. and Sazavsky, P. and Kiselova, M. and Selucky, P. and Bezdicka, P. and Journeau, C. and Piluso, P.Experimental investigation and thermodynamic simulation of the uranium-oxide-zirconium oxide-iron oxide system in air, Glass Physics and Chemistry, 37 (2011) 212-229.

477 Table 1. Compositions of the initial samples and heating conditions.

Component	Molar ratio			Heating condition			
	U/U+Zr	U+Zr/Fe+Cr	Fe/Fe+Cr	Atmosphere	Log $P(O_2)$	Temperature [K]	Time [h]
UO_2-Fe	1	1	1	Ar+10%H_2	-13.7	1473	2, 4, 8
						1673	2
				Ar+2%O_2	-1.7	1473	2, 4, 8
						1673	2
UO_2-Cr	1	1	0	Ar+10%H_2,	-13.7	1473	2, 4, 8
						1673	2
				Ar+2%O_2	-1.7	1473	2, 4, 8
						1673	2
U_3O_8-Cr_2O_3	1	1	0	Ar	-7.0	1473	2
UO_2-Fe-Cr	1	1	0.25, 0.5, 0.75, 0.9	Ar+10%H_2	-13.7	1473	24
				Ar+2%O_2	-1.7		
UO_2-SS	1	1	0.79	Ar+10%H_2	-13.7	1473	2, 4, 8
						1673	2
				Ar+2%O_2	-1.7	1473	2, 4, 8
						1673	2
UO_2-ZrO_2-SS	0.5	1	0.79	Ar+10%H_2,	-13.7	1473	2, 4, 8
						1673	2
				Ar+2%O_2	-1.7	1473	2, 4, 8

478

479

480

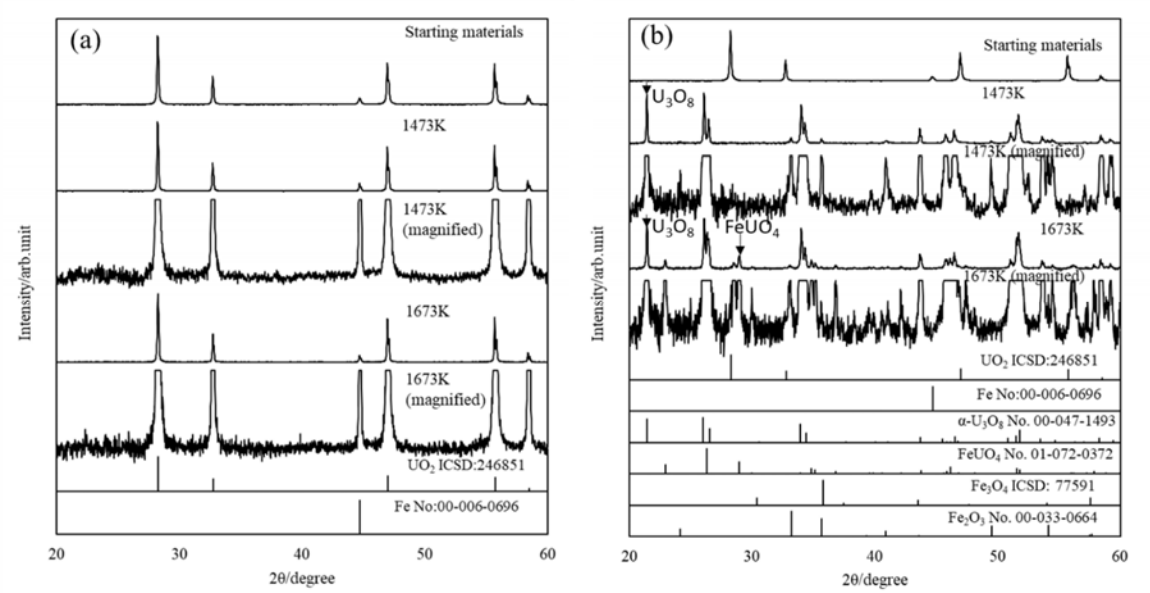

481

482 Fig. 1. XRD patterns of samples before and after heat treatment at 1473 and 1673 K in the

483 UO_2–Fe system under (a) the reducing condition and (b) the oxidizing condition.

484

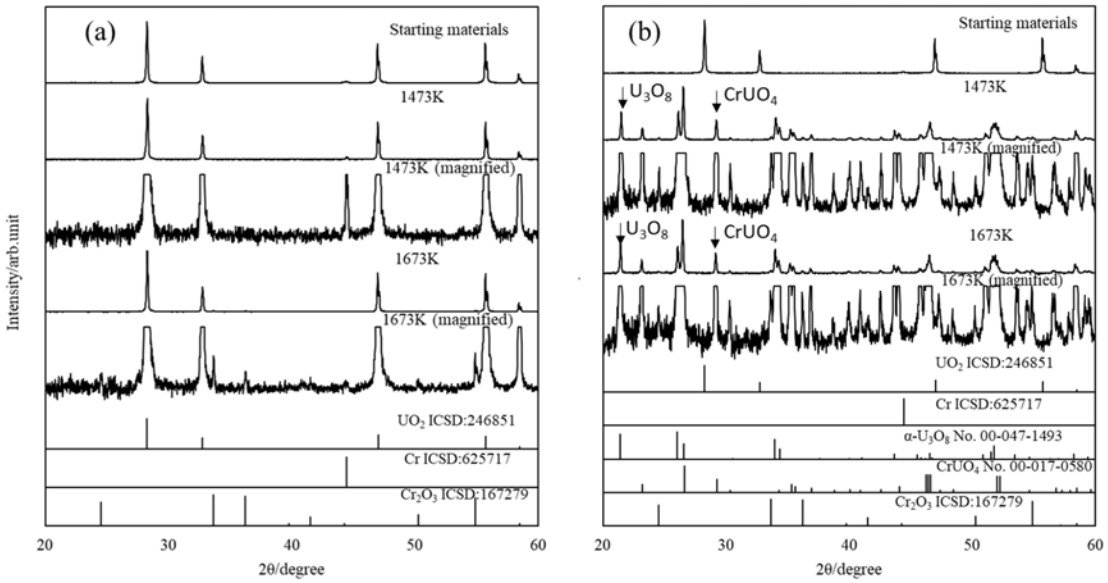

485

486 Fig. 2. XRD patterns of samples before and after heat treatment at 1473 and 1673 K in the

487 UO_2–Cr system under (a) the reducing condition and (b) the oxidizing condition

488

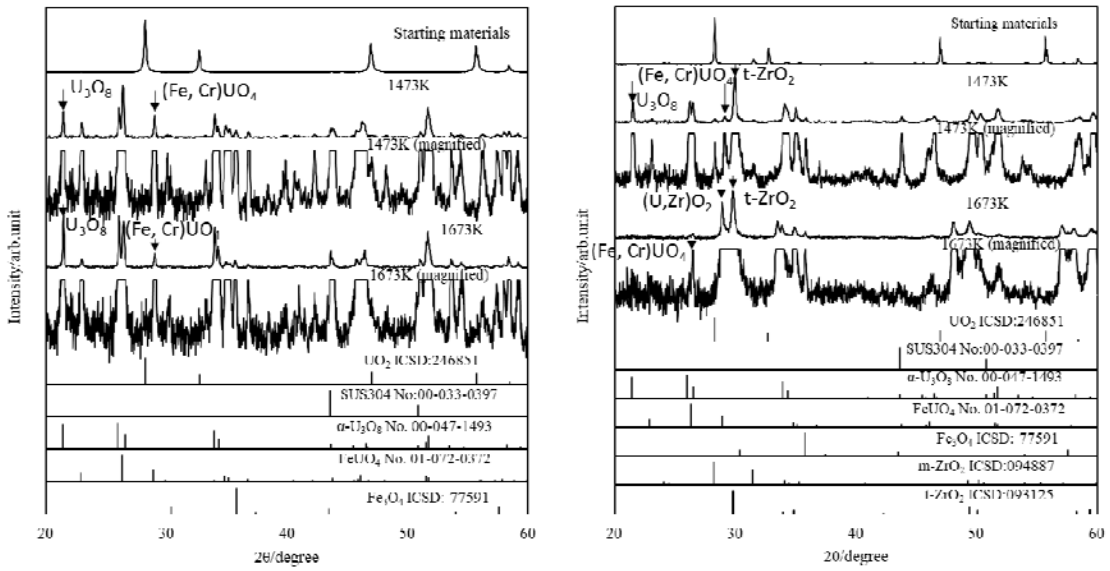

Fig. 3. XRD patterns of samples (a) in the UO_2–SS system and (b) in the UO_2–ZrO_2–SS system before and after heat-treatment at 1473 and 1673 K under the oxidizing condition.

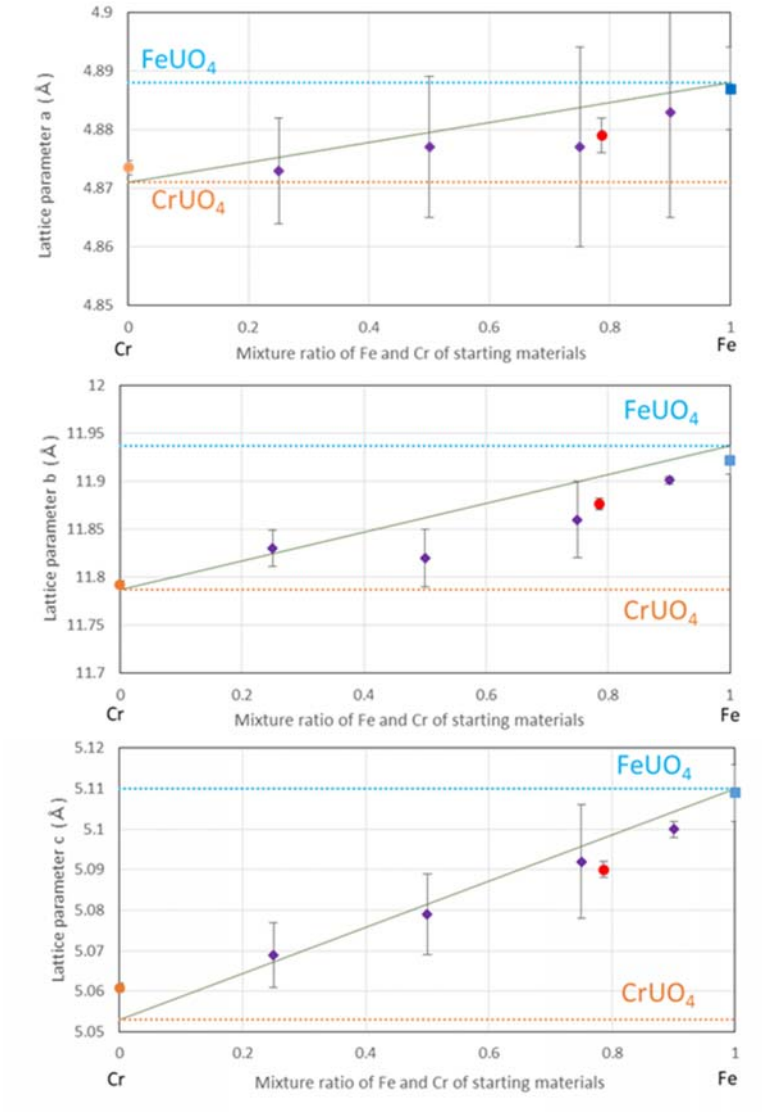

493

494 Fig. 4. Lattice parameters (*a*, *b*, *c*) of orthorhombic $FeUO_4$, $CrUO_4$, and $(Fe_x, Cr_{1-x})UO_4$

495 $(0.25 \leq x \leq 0.9)$.

496

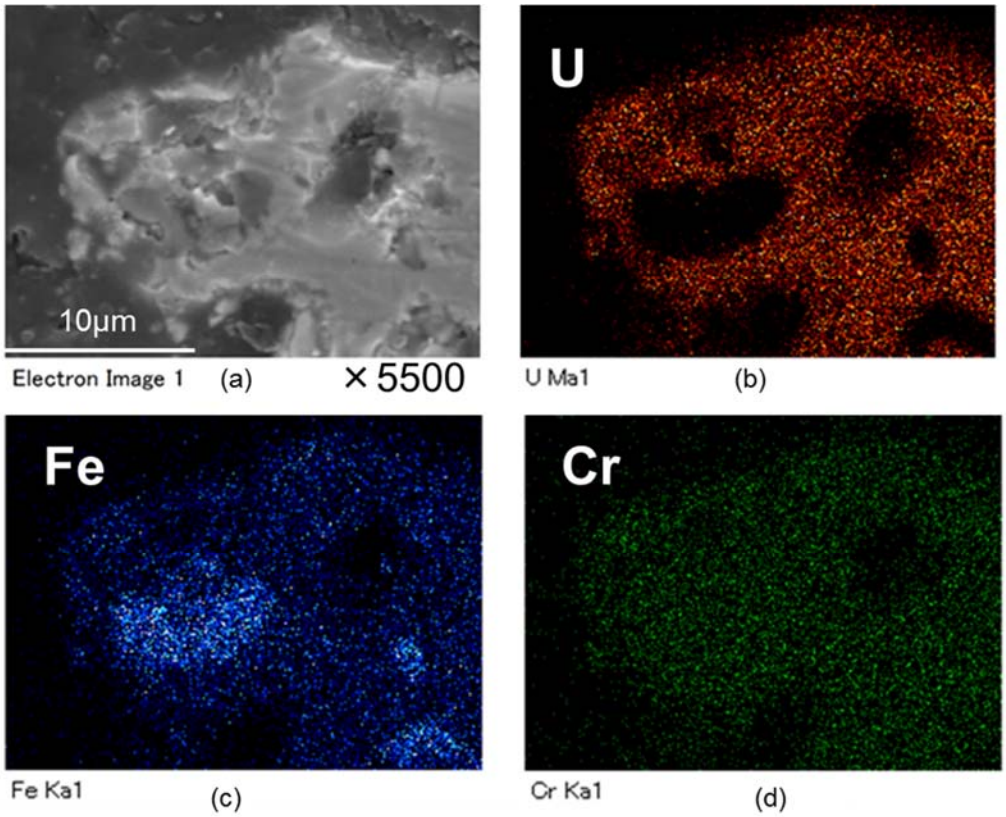

497

498 Fig. 5. SEM and X-ray mapping images of U, Fe, and Cr in UO_2–SS system after heat

499 treatment at 1473 K under the oxidizing condition for 24 h.

500

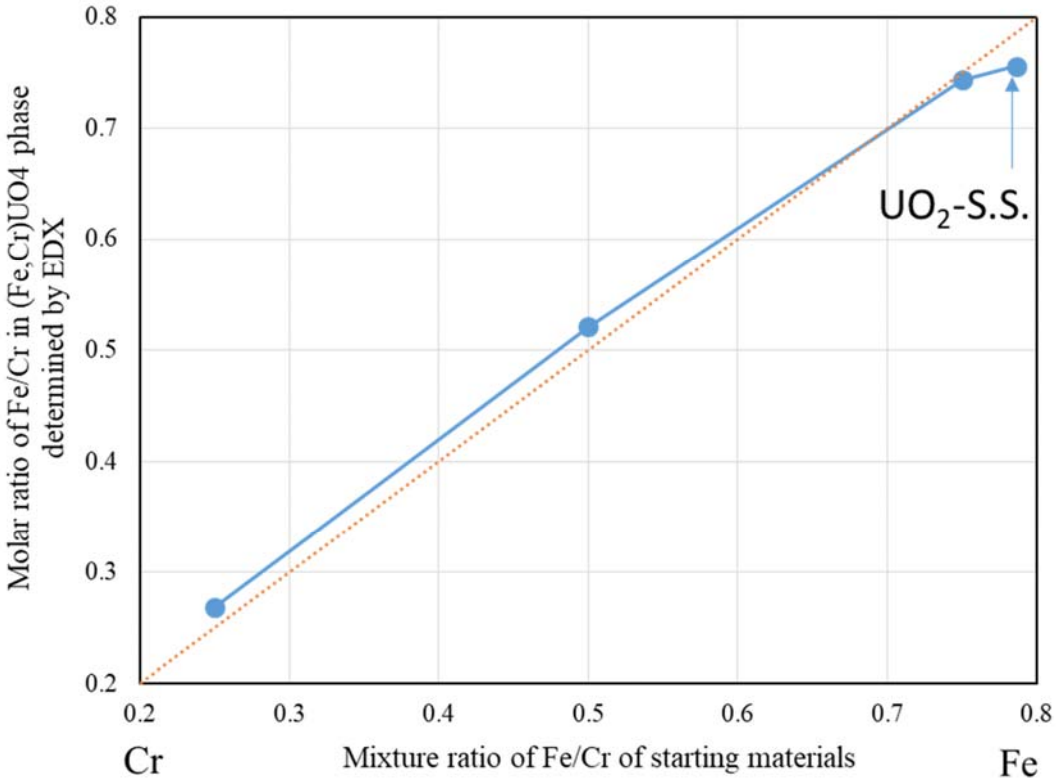

Fig. 6. Fe/Cr ratio of (Fe_x, Cr_{1-x})UO_4 ($0 < x < 1$) obtained by EDX analysis versus mixture ratio of Fe/Cr in starting materials.

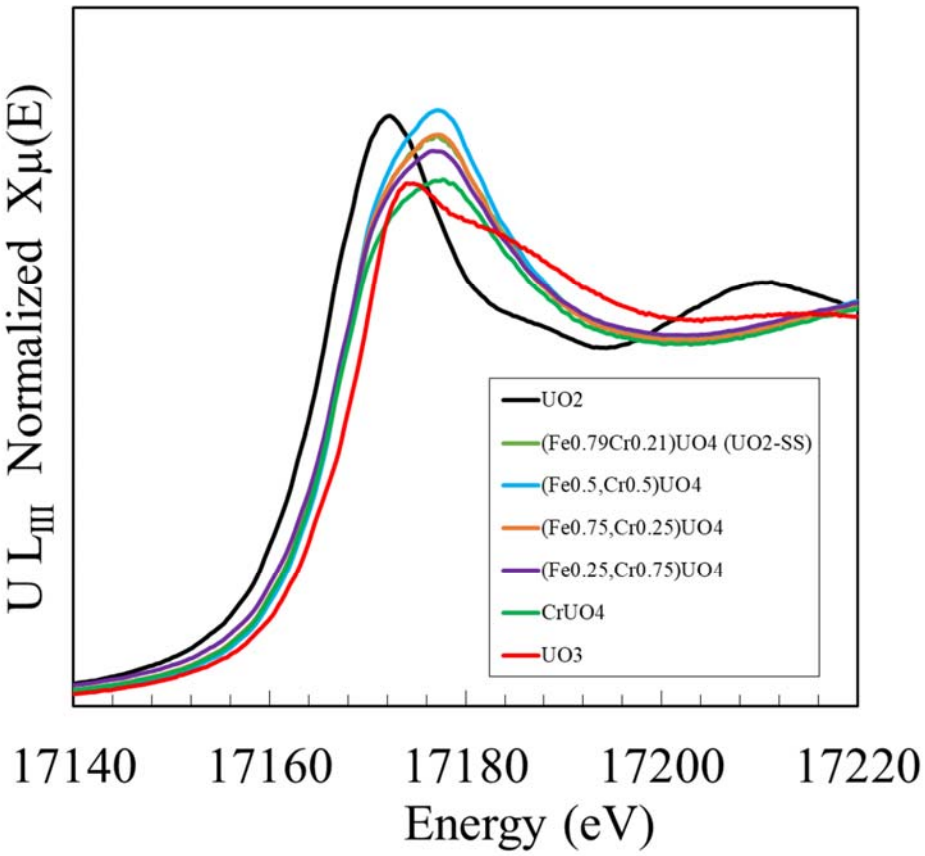

505

506 Fig. 7. U L_{III} XANES spectra of (Fe_x, Cr_{1-x})UO_4 and $CrUO_4$ samples.

507